Weierstraß-Institut
für Angewandte Analysis und Stochastik
Leibniz-Institut im Forschungsverbund Berlin e. V.

Preprint ISSN 2198-5855

Pressure-robust $L^2(\Omega)$ error analysis for Raviart–Thomas enriched Scott–Vogelius pairs

Volker John[1,2], Xu Li[3], Christian Merdon[1]

submitted: March 22, 2024

[1] Weierstraß-Institut
Mohrenstr. 39
10117 Berlin
Germany
E-Mail: volker.john@wias-berlin.de
christian.merdon@wias-berlin.de

[2] Department of Mathematics and Computer Science
Freie Universität Berlin
Arnimallee 6
14195 Berlin
Germany

[3] Eastern Institute for Advanced Study
Eastern Institute of Technology
Tongxin Road 568
315200 Ningbo
P. R. China

No. 3097
Berlin 2024

2020 *Mathematics Subject Classification.* 65N15, 65N30, 76M10.

2010 *Physics and Astronomy Classification Scheme.* 47.10.ad, 47.11.Fg.

Key words and phrases. Stokes equations, finite element method, stabilization, divergence-free, pressure-robust L^2 velocity error analysis .

Edited by
Weierstraß-Institut für Angewandte Analysis und Stochastik (WIAS)
Leibniz-Institut im Forschungsverbund Berlin e. V.
Mohrenstraße 39
10117 Berlin
Germany

Fax: +49 30 20372-303
E-Mail: preprint@wias-berlin.de
World Wide Web: http://www.wias-berlin.de/

Pressure-robust $L^2(\Omega)$ error analysis for Raviart–Thomas enriched Scott–Vogelius pairs

Volker John, Xu Li, Christian Merdon

Abstract

Recent work shows that it is possible to enrich the Scott–Vogelius finite element pair by certain Raviart–Thomas functions to obtain an inf-sup stable and divergence-free method on general shape-regular meshes. A skew-symmetric consistency term was suggested for avoiding an additional stabilization term for higher order elements, but no $L^2(\Omega)$ error estimate was shown for the Stokes equations. This note closes this gap. In addition, the optimal choice of the stabilization parameter is studied numerically.

1 Introduction

This paper is concerned with a class of inf-sup stabilized Scott–Vogelius element methods introduced in [6] for the Stokes equations

$$\begin{aligned} -\nu\Delta\boldsymbol{u} + \nabla p &= \boldsymbol{f} && \text{in } \Omega, \\ \operatorname{div}(\boldsymbol{u}) &= 0 && \text{in } \Omega, \\ \boldsymbol{u} &= \boldsymbol{0} && \text{on } \partial\Omega. \end{aligned} \tag{1.1}$$

Here $\Omega \subset \mathbb{R}^d$, $d \in \{2,3\}$, is a bounded domain with polyhedral Lipschitz boundary $\partial\Omega$, $\nu > 0$ is the constant viscosity coefficient, and $\boldsymbol{f} \in \boldsymbol{L}^2(\Omega)$ denotes the external body force. The unknowns are the velocity field $\boldsymbol{u}$ and the pressure p.

A velocity-pressure finite element pair is called divergence-free if it preserves the divergence-free property in the sense of $L^2(\Omega)$, such as the well-known Scott–Vogelius pairs [10]. The construction of the Scott–Vogelius elements is quite straightforward: Its velocity space consists of vector-valued continuous piecewise polynomials with order k, while the corresponding pressure space consists of discontinuous piecewise polynomials with order $k-1$ (namely $\boldsymbol{P}_k \times P_{k-1}^{\mathrm{disc}}$). Moreover, as a class of divergence-free methods, it has many appealing properties which have been extensively studied in the literature, e.g., [7, 5, 9, 4, 1]. However, it is also well known that the stability condition of the Scott–Vogelius pairs is not mild especially in three dimensions: It is only inf-sup stable on some special types of meshes with $k \geqslant d$ or $k \geqslant 2d$, e.g., see [11, 12].

Recently, in [8, 6], the authors proposed a new strategy for inf-sup stabilizing Scott–Vogelius pairs with arbitrary order on general shape-regular simplicial meshes. Therein a suitable subspace of the classical Raviart–Thomas space of order $k-1$ was chosen to enrich the $\boldsymbol{P}_k$ velocity space. For $k < d$, the

DOI 10.20347/WIAS.PREPRINT.3097

enrichment involves also lowest-order Raviart–Thomas functions that need to be stabilized. The novel discrete formulation does not involve any face integrals although the Raviart–Thomas elements are tangentially discontinuous across interior faces. The resulting scheme is stable and still divergence-free. Moreover, it is shown that the scheme can be reduced to a $\boldsymbol{P}_k \times P_0$ one for arbitrary k, that is, all unknowns related to the enrichment part and higher-order pressures can be removed in the solution process and then obtained by an inexpensive post-processing. However, since the velocity-velocity bilinear form given in [6] is not symmetric except for the lowest order case, it is clear that for deriving an optimal $L^2(\Omega)$ error estimate the standard duality argument technique has to be augmented, which was not done in [6].

The main object of this paper is to provide an optimal $L^2(\Omega)$ error estimate for the enriched Scott–Vogelius pairs, i.e.,

$$\|\boldsymbol{u} - \boldsymbol{u}_h\| \lesssim h^{k+1} |\boldsymbol{u}|_{\boldsymbol{H}^{k+1}(\Omega)}.$$

The estimate reflects the pressure-robustness of the scheme as it is pressure-independent and the generic constant hidden in $\lesssim$ depends on the shape-regularity of the mesh, but not on the mesh width h or the viscosity ν. To obtain this result the usual dual estimate approach has to be complemented with some estimate for the skew-symmetric part of the involved bilinear form. Since for $k < d$ the hidden generic constant above also depends on the stabilization parameter for the lowest-order Raviart–Thomas part of the enrichment, numerical studies are presented that investigate the optimal choice of this stabilization parameter.

The paper is organized as follows. In Section 2 the enriched Scott–Vogelius element method from [6] is briefly recalled. An optimal a priori $L^2(\Omega)$ error estimate is given in Section 3. Section 4 is devoted to the numerical studies.

2 The inf-sup stabilized Scott–Vogelius finite element method

Standard notation for Lebesgue and Sobolev spaces is used. The inner product in $L^2(\Omega)$ and $\boldsymbol{L}^2(\Omega)$ is denoted by $(\cdot, \cdot)$ and the induced norm by $\|\cdot\|$. The symbol $\lesssim$ is used for estimates where the constant does not depend on the mesh width and the viscosity.

The finite element velocity space is given by $\boldsymbol{V}_h := \boldsymbol{V}_h^{\mathrm{ct}} \times \boldsymbol{V}_h^{\mathrm{R}}$ on a shape-regular simplicial triangulation $\mathcal{T}_h$, where $\boldsymbol{V}_h^{\mathrm{ct}} := \boldsymbol{P}_k \cap \boldsymbol{H}_0^1(\Omega)$ and $\boldsymbol{V}_h^{\mathrm{R}} \subseteq \boldsymbol{RT}_{k-1}$ is the enrichment space contained in the Raviart–Thomas space of order $k-1$. For $k = 1$, $\boldsymbol{V}_h^{\mathrm{R}}$ consists of the functions in the lowest order Raviart–Thomas space RT_0 with vanishing normal boundary values, while for $k \geqslant d$, $\boldsymbol{V}_h^{\mathrm{R}}$ consists of some higher order Raviart–Thomas cell bubbles. The details of the construction of $\boldsymbol{V}_h^{\mathrm{R}}$ can be found in [6]. The corresponding space of discretely divergence-free functions reads

$$\boldsymbol{V}_{h,\mathrm{div}} := \left\{\boldsymbol{v}_h = \left(\boldsymbol{v}_h^{\mathrm{ct}}, \boldsymbol{v}_h^{\mathrm{R}}\right) \in \boldsymbol{V}_h : \operatorname{div}\left(\boldsymbol{v}_h^{\mathrm{ct}} + \boldsymbol{v}_h^{\mathrm{R}}\right) = 0\right\}.$$

Then, the finite element problem can be formulated in $\boldsymbol{V}_{h,\mathrm{div}}$: Find $\boldsymbol{u}_h \in \boldsymbol{V}_{h,\mathrm{div}}$ such that

$$a_h\left(\boldsymbol{u}_h, \boldsymbol{v}_h\right) = \left(\nu^{-1}\boldsymbol{f}, \boldsymbol{v}_h^{\mathrm{ct}} + \boldsymbol{v}_h^{\mathrm{R}}\right) \quad \text{for all } \boldsymbol{v}_h \in \boldsymbol{V}_{h,\mathrm{div}}, \tag{2.1}$$

where the bilinear form is defined by

$$a_h(\boldsymbol{u}_h, \boldsymbol{v}_h) := \left(\nabla \boldsymbol{u}_h^{\mathrm{ct}}, \nabla \boldsymbol{v}_h^{\mathrm{ct}}\right) - \left(\Delta_{\mathrm{pw}} \boldsymbol{u}_h^{\mathrm{ct}}, \boldsymbol{v}_h^{\mathrm{R}}\right) + \left(\Delta_{\mathrm{pw}} \boldsymbol{v}_h^{\mathrm{ct}}, \boldsymbol{u}_h^{\mathrm{R}}\right) + a_h^{\mathrm{D}}\left(\boldsymbol{u}_h^{\mathrm{RT}_0}, \boldsymbol{v}_h^{\mathrm{RT}_0}\right).$$

Here, Δ_{pw} is a piecewise defined Laplacian, a_h^{D} is a stabilization term, and $\boldsymbol{u}_h^{\mathrm{RT}_0}$ is the part of $\boldsymbol{u}_h^{\mathrm{R}}$ that is contained in RT_0. It can be identified by $\boldsymbol{u}_h^{\mathrm{RT}_0} = I_{\mathrm{RT}_0} \boldsymbol{u}_h^{\mathrm{R}}$ where I_{RT_0} is the standard interpolator into RT_0. It is worth mentioning that, $I_{\mathrm{RT}_0} \boldsymbol{u}_h^{\mathrm{R}}$ is zero exactly for $k \geqslant d$, which means the method is parameter-free in this case.

Let h denote the maximal diameter of the mesh cells of $\mathcal{T}_h$ and let $h_{\mathcal{T}}$ be a piecewise constant function that takes on each mesh cell the corresponding diameter of the cell. For the analysis, the only requirement is the equivalence

$$a_h^{\mathrm{D}}\left(\boldsymbol{v}_h^{\mathrm{RT}_0}, \boldsymbol{v}_h^{\mathrm{RT}_0}\right) \approx \left\| h_{\mathcal{T}}^{-1} \boldsymbol{v}_h^{\mathrm{RT}_0} \right\|^2. \tag{2.2}$$

The bilinear form a_h can be extended continuously to the space $\boldsymbol{V}^+ \times \boldsymbol{V}_h^{\mathrm{R}}$ with

$$\boldsymbol{V}^+ := \left\{ \boldsymbol{v} \in \boldsymbol{H}_0^1(\Omega) : \forall T \in \mathcal{T}, \Delta|_T \boldsymbol{v} \in L^2(T) \right\}.$$

In this product space, the velocity of the exact solution $(\boldsymbol{u}, p) \in \boldsymbol{V} \times Q := \boldsymbol{H}_0^1(\Omega) \times L_0^2(\Omega)$ is identified with $(\boldsymbol{u}, \boldsymbol{0})$. The subspace of divergence-free functions reads

$$\boldsymbol{V}_0^+ = \{ \boldsymbol{v} = (\boldsymbol{v}^{\mathrm{ct}}, \boldsymbol{0}) : \boldsymbol{v}^{\mathrm{ct}} \in \boldsymbol{V}^+ \text{ and } \operatorname{div}(\boldsymbol{v}^{\mathrm{ct}}) = 0 \}.$$

Consistency of the method is proven in [6, Lemma 5.1] for $\boldsymbol{u} \in \boldsymbol{V}_0^+$, i.e., it holds that

$$a_h(\boldsymbol{u}, \boldsymbol{v}) = \left(\nu^{-1} \boldsymbol{f}, \boldsymbol{v}^{\mathrm{ct}} + \boldsymbol{v}^{\mathrm{R}}\right) \quad \text{for all } \boldsymbol{v} \in \boldsymbol{V}_0^+ + \boldsymbol{V}_{h,\mathrm{div}}, \tag{2.3}$$

which implies the Galerkin orthogonality

$$a_h(\boldsymbol{u} - \boldsymbol{u}_h, \boldsymbol{v}_h) = 0 \quad \text{for all } \boldsymbol{v}_h \in \boldsymbol{V}_{h,\mathrm{div}}. \tag{2.4}$$

In [6], the error analysis was performed in the norm

$$|||\boldsymbol{v}|||_\star^2 := |||\boldsymbol{v}|||^2 + \left\| h_{\mathcal{T}} \Delta_{\mathrm{pw}} \boldsymbol{v}^{\mathrm{ct}} \right\|^2 + \left\| \operatorname{div}\left((1 - I_{\mathrm{RT}_0}) \boldsymbol{v}^{\mathrm{R}} \right) \right\|^2 \quad \text{with } |||\boldsymbol{v}|||^2 := a_h(\boldsymbol{v}, \boldsymbol{v}) \tag{2.5}$$

for all $\boldsymbol{v} \in \boldsymbol{V}^+ \times \boldsymbol{V}_h^{\mathrm{R}}$. The following error estimate was shown in [6].

Theorem 2.1 (Pressure-robust velocity error estimate in the norm $|||\cdot|||_\star$) *Let $\boldsymbol{u} \in \boldsymbol{V}^+$ be the weak velocity solution of (1.1) and $\boldsymbol{u}_h \in \boldsymbol{V}_{h,\mathrm{div}}$ the discrete velocity solution of (2.1). Then it holds for a shape-regular family of triangulations $\{\mathcal{T}_h\}$ that* [1]

$$\begin{aligned} |||(\boldsymbol{u}, \boldsymbol{0}) - \boldsymbol{u}_h|||_\star &\lesssim \inf_{\boldsymbol{v}_h \in \boldsymbol{V}_{h,\mathrm{div}}} |||(\boldsymbol{u}, \boldsymbol{0}) - \boldsymbol{v}_h|||_\star \\ &\leqslant \inf_{\boldsymbol{v}_h^{\mathrm{ct}} \in \boldsymbol{V}_h^{\mathrm{ct}}} \left\{ (1 + C_F) \|\nabla(\boldsymbol{u} - \boldsymbol{v}_h^{\mathrm{ct}})\| + \|h_{\mathcal{T}} \Delta_{\mathrm{pw}} (\boldsymbol{u} - \boldsymbol{v}_h^{\mathrm{ct}})\| \right\}, \end{aligned} \tag{2.6}$$

[1] The term $\|h_{\mathcal{T}} \Delta_{\mathrm{pw}}(\boldsymbol{u} - \boldsymbol{v}_h^{\mathrm{ct}})\|$ in second inequality in (2.6) was missing in [6, Theorem 5.1].

where C_F is the stability constant of a Fortin interpolator which is characterized by (2.8) below. Additionally, if $\boldsymbol{u} \in \boldsymbol{H}^{\ell+1}(\Omega)$ with $1 \leqslant \ell \leqslant k$, one obtains the error estimate

$$|||(\boldsymbol{u}, \boldsymbol{0}) - \boldsymbol{u}_h|||_\star \lesssim h^\ell |\boldsymbol{u}|_{\boldsymbol{H}^{\ell+1}(\Omega)}. \tag{2.7}$$

Proof The first inequality in estimate (2.6) has been proved in [6, Theorem 5.1]. Let us prove the second one and (2.7). Let $\Pi : \boldsymbol{V} \to \boldsymbol{V}_h$ be a Fortin operator satisfying (see [6, Section 4])

$$|||\Pi \boldsymbol{v}|||_\star \leqslant C_F \|\nabla \boldsymbol{v}\| \quad \text{and} \quad (\operatorname{div}(\Pi \boldsymbol{v}), q_h) = (\operatorname{div}(\boldsymbol{v}), q_h) \quad \text{for all } \boldsymbol{v} \in \boldsymbol{V}, q_h \in Q_h, \tag{2.8}$$

where $C_F > 0$ is a positive constant which is independent of h, and $Q_h \subset Q$ is indeed the pressure space consisting of the discontinuous piecewise polynomials of degree no more than $k-1$. Note that $\operatorname{div}(\boldsymbol{V}_h^{\mathrm{ct}}) \subseteq Q_h$. Let $\boldsymbol{w}_h^{\mathrm{ct}} \in \boldsymbol{V}_h^{\mathrm{ct}}$ be arbitrary, $\boldsymbol{w}_h = (\boldsymbol{w}_h^{\mathrm{ct}}, \boldsymbol{0}) \in \boldsymbol{V}_h$ and $\boldsymbol{v}_h = \boldsymbol{w}_h + \Pi(\boldsymbol{u} - \boldsymbol{w}_h^{\mathrm{ct}}) \in \boldsymbol{V}_h$ with $\boldsymbol{u}$ being the weak velocity solution of (1.1). From the equality in (2.8) one has $\boldsymbol{v}_h \in \boldsymbol{V}_{h,\mathrm{div}}$. It follows from a triangle inequality, the estimate in (2.8), and the definition of $|||\bullet|||_\star$ (see (2.5)) that

$$\begin{aligned} |||(\boldsymbol{u}, \boldsymbol{0}) - \boldsymbol{v}_h|||_\star &\leqslant |||(\boldsymbol{u}, \boldsymbol{0}) - \boldsymbol{w}_h|||_\star + |||\Pi(\boldsymbol{u} - \boldsymbol{w}_h^{\mathrm{ct}})|||_\star \\ &\leqslant |||(\boldsymbol{u}, \boldsymbol{0}) - \boldsymbol{w}_h|||_\star + C_F \|\nabla(\boldsymbol{u} - \boldsymbol{w}_h^{\mathrm{ct}})\| \\ &= (1 + C_F)\|\nabla(\boldsymbol{u} - \boldsymbol{w}_h^{\mathrm{ct}})\| + \|h_\mathcal{T} \Delta_{\mathrm{pw}}(\boldsymbol{u} - \boldsymbol{w}_h^{\mathrm{ct}})\|. \end{aligned}$$

Since $\boldsymbol{w}_h^{\mathrm{ct}}$ is arbitrary, taking infimums on both side of the above estimate yields the second inequality in (2.6). Then (2.7) follows immediately from the approximation properties of $\boldsymbol{V}_h^{\mathrm{ct}}$ (e.g., see [2, Theorem 4.4.4]). This completes the proof. □

Moreover, the following estimate is needed in the subsequent analysis.

Lemma 2.2 *For any $\boldsymbol{v}_h^{\mathrm{R}} \in \boldsymbol{V}_h^{\mathrm{R}}$ it holds that*

$$\left\| h_\mathcal{T}^{-1} \boldsymbol{v}_h^{\mathrm{R}} \right\| \lesssim |||(\boldsymbol{0}, \boldsymbol{v}_h^{\mathrm{R}})|||_\star \tag{2.9}$$

Proof Recall that $\boldsymbol{v}_h^{\mathrm{R}}$ can be uniquely decomposed into

$$\boldsymbol{v}_h^{\mathrm{R}} = \boldsymbol{v}_h^{\mathrm{RT}_0} + \tilde{\boldsymbol{v}}_h^{\mathrm{R}} \in \boldsymbol{RT}_0 \oplus \widetilde{\boldsymbol{RT}}_{k-1}^{\mathrm{int}}(\mathcal{T}),$$

where $\boldsymbol{v}_h^{\mathrm{RT}_0}$ is exactly $I_{\mathrm{RT}_0} \boldsymbol{v}_h^{\mathrm{R}}$ and $\widetilde{\boldsymbol{RT}}_{k-1}^{\mathrm{int}}(\mathcal{T})$ is a space defined in [6] whose exact form is not of importance for this note. The triangle inequality implies $\|h_\mathcal{T}^{-1} \boldsymbol{v}_h^{\mathrm{R}}\| \leqslant \|h_\mathcal{T}^{-1} \boldsymbol{v}_h^{\mathrm{RT}_0}\| + \|h_\mathcal{T}^{-1} \tilde{\boldsymbol{v}}_h^{\mathrm{R}}\|$. The equivalence (2.2) and [6, Lemma 5.2] show

$$\left\| h_\mathcal{T}^{-1} \boldsymbol{v}_h^{\mathrm{RT}_0} \right\| \lesssim a_h^{\mathrm{D}} \left(\boldsymbol{v}_h^{\mathrm{RT}_0}, \boldsymbol{v}_h^{\mathrm{RT}_0} \right)^{1/2} \quad \text{and} \quad \left\| h_\mathcal{T}^{-1} \tilde{\boldsymbol{v}}_h^{\mathrm{R}} \right\| \lesssim \left\| \operatorname{div}(\tilde{\boldsymbol{v}}_h^{\mathrm{R}}) \right\|.$$

Then, it follows from (2.5) that

$$|||(\boldsymbol{0}, \boldsymbol{v}_h^{\mathrm{R}})|||_\star^2 = a_h^{\mathrm{D}} \left(\boldsymbol{v}_h^{\mathrm{RT}_0}, \boldsymbol{v}_h^{\mathrm{RT}_0} \right) + \left\| \operatorname{div}(\tilde{\boldsymbol{v}}_h^{\mathrm{R}}) \right\|^2 \gtrsim \left\| h_\mathcal{T}^{-1} \boldsymbol{v}_h^{\mathrm{R}} \right\|^2.$$

This completes the proof. □

3 Error analysis in the $L^2(\Omega)$ norm

The error analysis in $\boldsymbol{L}^2(\Omega)$ is based on the Aubin–Nitsche trick. To this end, consider, for given $\boldsymbol{r} \in \boldsymbol{L}^2(\Omega)$, the dual problem to (1.1)

$$-\Delta \boldsymbol{u}_r - \nabla p_r = \boldsymbol{r}, \quad \operatorname{div}(\boldsymbol{u}_r) = 0 \quad \text{in } \Omega, \quad \boldsymbol{u}_r = \boldsymbol{0} \quad \text{on } \partial\Omega, \tag{3.1}$$

where the weak solution is denoted by $(\boldsymbol{u}_r, p_r) \in \boldsymbol{V} \times Q$. As usual, one has to assume regularity of the velocity solution, i.e., $\boldsymbol{u}_r \in \boldsymbol{H}^2(\Omega)$, together with the stability bound

$$\|\boldsymbol{u}_r\|_{\boldsymbol{H}^2(\Omega)} \lesssim \|\boldsymbol{r}\|. \tag{3.2}$$

This property holds for convex polyhedral domains in two and three dimensions, see, e.g., [3]. The corresponding finite element problem to (3.1) reads as follows: find $\boldsymbol{u}_{r,h} \in \boldsymbol{V}_{h,\mathrm{div}}$ such that

$$a_h\left(\boldsymbol{u}_{r,h}, \boldsymbol{v}_h\right) = \left(\boldsymbol{r}, \boldsymbol{v}_h^{\mathrm{ct}} + \boldsymbol{v}_h^{\mathrm{R}}\right) \quad \text{for all } \boldsymbol{v}_h \in \boldsymbol{V}_{h,\mathrm{div}}. \tag{3.3}$$

The key argument of the proof is an estimate of the skew-symmetric part of $a_h(\cdot,\cdot)$ defined by

$$a_{\mathsf{skew}}(\boldsymbol{u}_h, \boldsymbol{v}_h) := \frac{a_h(\boldsymbol{u}_h, \boldsymbol{v}_h) - a_h(\boldsymbol{v}_h, \boldsymbol{u}_h)}{2} = -\left(\Delta_{\mathsf{pw}} \boldsymbol{u}_h^{\mathrm{ct}}, \boldsymbol{v}_h^{\mathrm{R}}\right) + \left(\Delta_{\mathsf{pw}} \boldsymbol{v}_h^{\mathrm{ct}}, \boldsymbol{u}_h^{\mathrm{R}}\right). \tag{3.4}$$

Again, in the product space, the velocity solution $\boldsymbol{u}_r$ should be identified with $(\boldsymbol{u}_r, \boldsymbol{0})$.

Theorem 3.1 (Pressure-robust velocity error estimate in $\boldsymbol{L}^2(\Omega)$) *Let $\{\mathcal{T}_h\}$ be a family of shape-regular triangulations and let the regularity assumption (3.2) hold. The $\boldsymbol{L}^2(\Omega)$ error between the weak velocity solution $\boldsymbol{u}$ of (1.1) and the discrete solution $\boldsymbol{u}_h$ of (2.1) is bounded by*

$$\|\boldsymbol{u} - \boldsymbol{u}_h^{\mathrm{s}}\| \lesssim h |||(\boldsymbol{u}, 0) - \boldsymbol{u}_h|||_\star. \tag{3.5}$$

Here, $\boldsymbol{u}_h^{\mathrm{s}} := \boldsymbol{u}_h^{\mathrm{ct}} + \boldsymbol{u}_h^{\mathrm{R}}$ denotes the sum of all velocity components (while $\boldsymbol{u}_h = (\boldsymbol{u}_h^{\mathrm{ct}}, \boldsymbol{u}_h^{\mathrm{R}})$ denotes the pair in the product space).

Proof By definition it is

$$\|\boldsymbol{u} - \boldsymbol{u}_h^{\mathrm{s}}\| = \sup_{\boldsymbol{r} \in \boldsymbol{L}^2(\Omega)} \frac{(\boldsymbol{r}, \boldsymbol{u} - \boldsymbol{u}_h^{\mathrm{s}})}{\|\boldsymbol{r}\|}. \tag{3.6}$$

For given $\boldsymbol{r} \in \boldsymbol{L}^2(\Omega)$, let $\boldsymbol{u}_r$ and $\boldsymbol{u}_{r,h}$ denote the solutions of (3.1) and (3.3), respectively. Applying the Galerkin orthogonality (2.4) and (3.4) gives

$$a_h\left(\boldsymbol{u}_{r,h}, \boldsymbol{u} - \boldsymbol{u}_h\right) = a_h\left(\boldsymbol{u}_{r,h}, \boldsymbol{u} - \boldsymbol{u}_h\right) - a_h\left(\boldsymbol{u} - \boldsymbol{u}_h, \boldsymbol{u}_{r,h}\right) = 2a_{\mathsf{skew}}\left(\boldsymbol{u}_{r,h}, \boldsymbol{u} - \boldsymbol{u}_h\right).$$

With this relation and the consistency property (2.3), one obtains for the numerator of (3.6)

$$\begin{aligned} (\boldsymbol{r}, \boldsymbol{u} - \boldsymbol{u}_h^{\mathrm{s}}) &= a_h(\boldsymbol{u}_r, \boldsymbol{u} - \boldsymbol{u}_h) = a_h(\boldsymbol{u}_r - \boldsymbol{u}_{r,h}, \boldsymbol{u} - \boldsymbol{u}_h) + a_h(\boldsymbol{u}_{r,h}, \boldsymbol{u} - \boldsymbol{u}_h) \\ &= a_h(\boldsymbol{u}_r - \boldsymbol{u}_{r,h}, \boldsymbol{u} - \boldsymbol{u}_h) + 2a_{\mathsf{skew}}\left(\boldsymbol{u}_{r,h}, \boldsymbol{u} - \boldsymbol{u}_h\right) =: A + B. \end{aligned}$$

Term A is a standard one. Applying a Cauchy–Schwarz inequality, using the definition (2.5) of the norm $|||\cdot|||_\star$, the error estimate (2.7) applied to the finite element problem (3.3) with $\ell = 1$, and the regularity assumption (3.2) yields

$$A = a_h(\boldsymbol{u}_r - \boldsymbol{u}_{r,h}, \boldsymbol{u} - \boldsymbol{u}_h) \lesssim |||\boldsymbol{u} - \boldsymbol{u}_h|||_\star |||\boldsymbol{u}_r - \boldsymbol{u}_{r,h}|||_\star \lesssim h|||\boldsymbol{u} - \boldsymbol{u}_h|||_\star \|\boldsymbol{r}\|. \tag{3.7}$$

The skew-symmetry of the stabilization requires to bound the additional term B. Utilizing (3.4), the Cauchy–Schwarz inequality, and Lemma 2.9 for $\boldsymbol{v}_h^{\mathrm{R}} = \boldsymbol{u}_h^{\mathrm{R}}$ leads to

$$\begin{aligned} B &= 2a_{\text{skew}}(\boldsymbol{u}_{r,h}, \boldsymbol{u} - \boldsymbol{u}_h) = \left(\Delta_{\text{pw}}\boldsymbol{u}_{r,h}^{\text{ct}}, \boldsymbol{u}_h^{\mathrm{R}}\right) + \left(\Delta_{\text{pw}}(\boldsymbol{u} - \boldsymbol{u}_h^{\text{ct}}), \boldsymbol{u}_{r,h}^{\mathrm{R}}\right) \\ &\lesssim \left(\left\|h_{\mathcal{T}}\Delta_{\text{pw}}(\boldsymbol{u} - \boldsymbol{u}_h^{\text{ct}})\right\| + \left\|h_{\mathcal{T}}^{-1}\boldsymbol{u}_h^{\mathrm{R}}\right\|\right)\left(\left\|h_{\mathcal{T}}\Delta_{\text{pw}}\boldsymbol{u}_{r,h}^{\text{ct}}\right\| + \left\|h_{\mathcal{T}}^{-1}\boldsymbol{u}_{r,h}^{\mathrm{R}}\right\|\right) \\ &\lesssim |||(\boldsymbol{u}, 0) - \boldsymbol{u}_h|||_\star \left(\left\|h_{\mathcal{T}}\Delta_{\text{pw}}\boldsymbol{u}_{r,h}^{\text{ct}}\right\| + \left\|h_{\mathcal{T}}^{-1}\boldsymbol{u}_{r,h}^{\mathrm{R}}\right\|\right). \end{aligned}$$

Using the triangle inequality, Theorem 2.1 for $\boldsymbol{u}_r$ with $\ell = 1$, Lemma 2.9 for $\boldsymbol{v}_h^{\mathrm{R}} = \boldsymbol{u}_{r,h}^{\mathrm{R}}$, and the regularity assumption (3.2) gives

$$\begin{aligned} \left\|h_{\mathcal{T}}\Delta_{\text{pw}}\boldsymbol{u}_{r,h}^{\text{ct}}\right\| + \left\|h_{\mathcal{T}}^{-1}\boldsymbol{u}_{r,h}^{\mathrm{R}}\right\| &\leqslant \left\|h_{\mathcal{T}}\Delta_{\text{pw}}(\boldsymbol{u}_{r,h}^{\text{ct}} - \boldsymbol{u}_r)\right\| + \left\|h_{\mathcal{T}}\Delta_{\text{pw}}\boldsymbol{u}_r\right\| + \left\|h_{\mathcal{T}}^{-1}\boldsymbol{u}_{r,h}^{\mathrm{R}}\right\| \\ &\lesssim |||\boldsymbol{u}_r - \boldsymbol{u}_{r,h}|||_\star + \left\|h_{\mathcal{T}}\Delta_{\text{pw}}\boldsymbol{u}_r\right\| \lesssim h\|\boldsymbol{u}_r\|_{\boldsymbol{H}^2(\Omega)} \lesssim h\|\boldsymbol{r}\|. \end{aligned}$$

Hence, we arrive at

$$B \lesssim h|||\boldsymbol{u} - \boldsymbol{u}_h|||_\star \|\boldsymbol{r}\| \tag{3.8}$$

Inserting (3.7) and (3.8) in (3.6) finishes the proof. □

4 Numerical studies

This section revisits the examples from [6] to study the impact of the RT_0 stabilization (that is only needed for $k \leqslant d$). In these studies we use

$$a_h^{\mathrm{D}}\left(\boldsymbol{u}_h^{\mathrm{RT}_0}, \boldsymbol{v}_h^{\mathrm{RT}_0}\right) := \alpha \sum_{F \in \mathcal{F}^0} \mathrm{dof}_F\left(\boldsymbol{u}_h^{\mathrm{RT}_0}\right) \mathrm{dof}_F\left(\boldsymbol{v}_h^{\mathrm{RT}_0}\right)\left(\mathrm{div}\boldsymbol{\psi}_F^{\mathrm{RT}_0}, \mathrm{div}\boldsymbol{\psi}_F^{\mathrm{RT}_0}\right), \tag{4.1}$$

which effectively penalizes the RT_0 part as it holds the equivalence (2.2) with equivalence constant scaled by α, see [8, Lemma 3.2] for a proof. Goals of the numerical experiments are to study the sensitivity of errors with respect to α and to find guidelines for an optimal choice of α.

4.1 Two-dimensional example

The first example is the stationary planar lattice flow on $\Omega = (0,1)^2$ defined by

$$\boldsymbol{u} = \begin{pmatrix} \sin(2\pi x)\sin(2\pi y) \\ \cos(2\pi x)\cos(2\pi y) \end{pmatrix} \quad \text{and} \quad p = \frac{1}{4}(\cos(4\pi x) - \cos(4\pi y)).$$

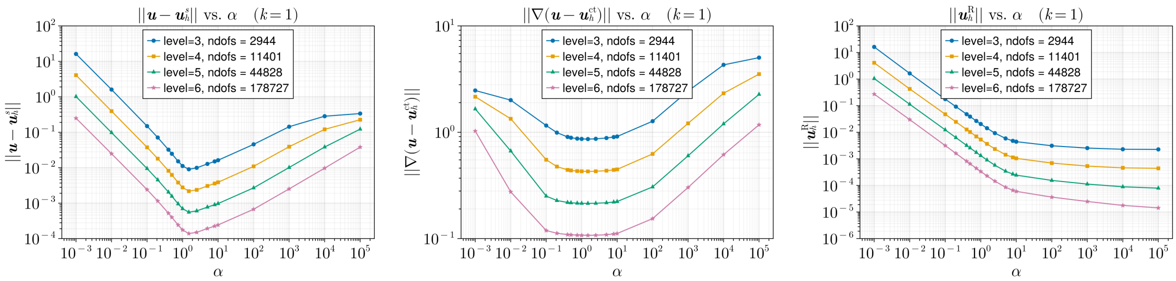

Figure 4.1: Dependence of the $L^2(\Omega)$ error (left), $H^1(\Omega)$ error (center) and the $L^2(\Omega)$ norm of the enrichment part (right) on the stabilization parameter α in the 2D example for order $k = 1$ on a series of unstructured meshes.

Table 4.1: Errors and convergence rates for $\alpha = 1$ and $k = 1$ in the 2D example on unstructured meshes.

ndof	$\|\|\boldsymbol{u} - \boldsymbol{u}_h^s\|\|$	rate	$\|\|\nabla(\boldsymbol{u} - \boldsymbol{u}_h^{\text{ct}})\|\|$	rate	$\|\|\boldsymbol{u}_h^{\text{R}}\|\|$	rate
145	2.995e-01	—	3.227e+00	—	3.767e-01	—
732	5.068e-02	2.19	1.773e+00	0.74	8.473e-02	1.84
2944	1.117e-02	2.17	8.653e-01	1.03	2.044e-02	2.04
11401	2.779e-03	2.05	4.295e-01	1.03	5.311e-03	1.99
44828	6.990e-04	2.02	2.147e-01	1.01	1.323e-03	2.03
178727	1.763e-04	1.99	1.075e-01	1.00	3.350e-04	1.99

The right-hand side $\boldsymbol{f}$ is chosen such that $(\boldsymbol{u}, p)$ solves the Stokes problem with $\nu = 10^{-6}$.

Figure 4.1 studies the dependence on several errors on the parameter α for the lowest-order scheme with $k = 1$. As expected, a larger value of the stabilization parameter α leads to a smaller enrichment part $\boldsymbol{u}_h^{\text{R}}$, but also to much larger errors. Vice versa, a small stabilization parameter α also leads to larger errors. Concerning the overall $L^2(\Omega)$ and $H^1(\Omega)$ errors of the velocity, the optimal parameter for α is in the interval $(1, 2)$ for all tested refinement levels. The convergence rates can be deduced from the multiplicative factor between the values of the plotted curves. The $L^2(\Omega)$ error plots show a factor of about 4 which corresponds to optimal quadratic convergence with respect to h for the full range of α. Table 4.1 shows the precise values for $\alpha = 1$.

Table 4.2: Errors and convergence rates for $\alpha = 1$ and $k = 1$ in the 3D example on unstructured meshes.

ndof	$\|\|\boldsymbol{u} - \boldsymbol{u}_h^s\|\|$	rate	$\|\|\nabla(\boldsymbol{u} - \boldsymbol{u}_h^{\text{ct}})\|\|$	rate	$\|\|\boldsymbol{u}_h^{\text{R}}\|\|$	rate
144	1.911e-01	—	1.715e+00	—	1.728e-01	—
729	1.433e-01	0.53	1.712e+00	0.00	1.016e-01	0.98
5210	4.539e-02	1.75	8.770e-01	1.02	3.146e-02	1.79
34113	1.210e-02	2.11	4.553e-01	1.05	9.292e-03	1.95
242743	2.920e-03	2.17	2.265e-01	1.07	2.331e-03	2.11

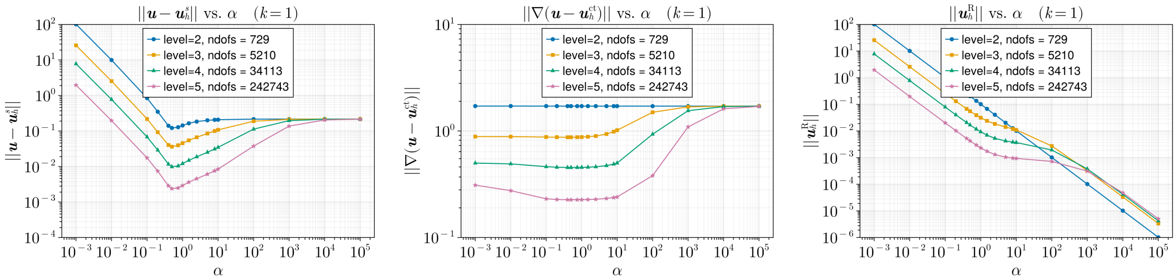

Figure 4.2: Dependence of the $L^2(\Omega)$ error (left), $H^1(\Omega)$ error (center) and the $L^2(\Omega)$ norm of the enrichment part (right) on the stabilization parameter α in the 3D example for order $k = 1$ on a series of unstructured meshes.

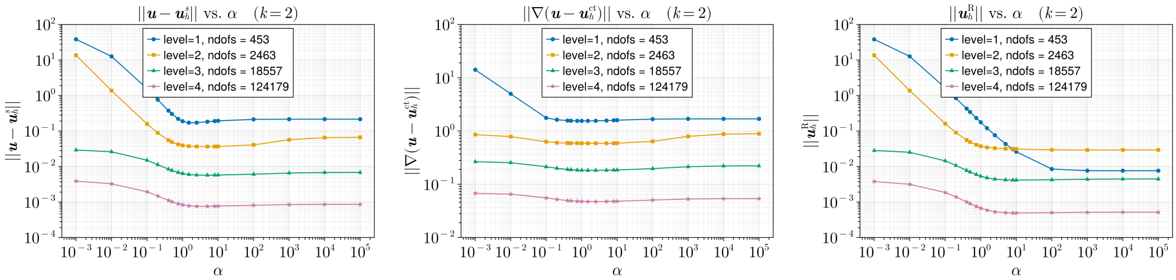

Figure 4.3: Dependence of the $L^2(\Omega)$ error (left), $H^1(\Omega)$ error (center) and the $L^2(\Omega)$ norm of the enrichment part (right) on the stabilization parameter α in the 3D example for order $k = 2$ on a series of unstructured meshes.

4.2 Three-dimensional example

In three dimensions consider the flow

$$\boldsymbol{u} = \frac{1}{2\pi}\,\mathrm{curl}\left\{[\sin(\pi x)\sin(\pi y)]^2 \sin(\pi z)\boldsymbol{e}_3\right\} \quad \text{and} \quad p = \sin(x)\sin(y)\sin(z) - (1-\cos 1)^3,$$

with $\boldsymbol{e}_3 = (0,0,1)^\top$. Again, $\boldsymbol{f}$ is chosen such that $(\boldsymbol{u}, p)$ solves the Stokes problem with $\nu = 10^{-6}$.

Figure 4.2 and Figure 4.3 study the dependence on several errors on the parameter α for the schemes with $k = 1$ and $k = 2$. The optimal value for α seems to be in the interval $\alpha \in [0.3, 1.0]$. Similar to the two-dimensional test case, the lowest order scheme ($k = 1$) with over-stabilization leads to a smaller enrichment part $\boldsymbol{u}_h^{\mathrm{R}}$, but also to larger errors. For $k = 2$ (which still includes an RT_0 enrichment part in three dimensions), over-stabilization does not seem to be as harmful as for $k = 1$. That might indicate that the RT_0 functions in the enrichment spaces are not really needed, at least on the grids that were used for the simulations. Tables 4.2 and 4.3 show the precise values for the errors and their convergence rates for $\alpha = 1$.

Table 4.3: Errors and convergence rates for $\alpha = 1$ and $k = 2$ in the 3D example on unstructured meshes.

ndof	$\|\|\boldsymbol{u} - \boldsymbol{u}_h^s\|\|$	rate	$\|\|\nabla(\boldsymbol{u} - \boldsymbol{u}_h^{\mathrm{ct}})\|\|$	rate	$\|\|\boldsymbol{u}_h^{\mathrm{R}}\|\|$	rate
453	1.883e-01	—	1.546e+00	—	1.762e-01	—
2463	3.927e-02	2.78	5.883e-01	1.71	3.737e-02	2.75
18557	6.349e-03	2.71	1.833e-01	1.73	5.359e-03	2.88
124179	8.321e-04	3.21	4.753e-02	2.13	6.685e-04	3.29
893527	1.048e-04	3.15	1.181e-02	2.12	8.581e-05	3.12

References

[1] N. Ahmed, G. R. Barrenechea, E. Burman, J. Guzmán, A. Linke, and C. Merdon. A pressure-robust discretization of Oseen's equation using stabilization in the vorticity equation. *SIAM J. Numer. Anal.*, 59(5):2746–2774, 2021.

[2] S. C. Brenner and L. R. Scott. *The mathematical theory of finite element methods*, volume 15 of *Texts in Applied Mathematics*. Springer, New York, third edition, 2008.

[3] M. Dauge. Stationary Stokes and Navier–Stokes systems on two- or three-dimensional domains with corners. Part I. linearized equations. *SIAM J. Math. Anal.*, 20(1):74–97, 1989.

[4] B. García-Archilla, V. John, and J. Novo. On the convergence order of the finite element error in the kinetic energy for high Reynolds number incompressible flows. *Comput. Methods Appl. Mech. Engrg.*, 385:Paper No. 114032, 54, 2021.

[5] V. John. *Finite element methods for incompressible flow problems*, volume 51 of *Springer Series in Computational Mathematics*. Springer, Cham, 2016.

[6] V. John, X. Li, C. Merdon, and H. Rui. Inf-sup stabilized Scott-Vogelius pairs on general shape-regular simplicial grids by Raviart–Thomas enrichment. *Math. Models Methods Appl. Sci.*, 2024 (published online).

[7] V. John, A. Linke, C. Merdon, M. Neilan, and L. G. Rebholz. On the divergence constraint in mixed finite element methods for incompressible flows. *SIAM Rev.*, 59(3):492–544, 2017.

[8] X. Li and H. Rui. A low-order divergence-free H(div)-conforming finite element method for Stokes flows. *IMA J. Numer. Anal.*, 42(4):3711–3734, 2022.

[9] P. W. Schroeder, C. Lehrenfeld, A. Linke, and G. Lube. Towards computable flows and robust estimates for inf-sup stable FEM applied to the time-dependent incompressible Navier–Stokes equations. *SeMA J.*, 75(4):629–653, 2018.

[10] L. R. Scott and M. Vogelius. Norm estimates for a maximal right inverse of the divergence operator in spaces of piecewise polynomials. *ESAIM: Math. Model. Numer. Anal. - Modélisation Mathématique et Analyse Numérique*, 19(1):111–143, 1985.

[11] S. Zhang. A new family of stable mixed finite elements for the 3D Stokes equations. *Math. Comp.*, 74(250):543–554, 2005.

[12] S. Zhang. Divergence-free finite elements on tetrahedral grids for $k \geqslant 6$. *Math. Comp.*, 80(274):669–695, 2011.